

# Hyperspectral Image Compression Based on DWT and TD with ALS Method

Kala Rajan<sup>1</sup> and Vasuki Murugesan<sup>2</sup>

<sup>1</sup>Department of Electronics and Communication Engineering, Sri Subramanya College of Engineering and Technology, India

<sup>2</sup>Department of Electronics and Communication Engineering, Velammal College of Engineering and Technology, India

**Abstract:** Compression of Hyper Spectral Image (HSI) is an important issue in remote sensing applications due to its huge data size. An efficient technique for HSI compression is proposed based on Discrete Wavelet Transform (DWT) and Tucker Decomposition (TD) with Adaptive Least Squares (ALS) method. This technique exploits both the spatial and spectral information in the images. ALS method is used to compute the TD which is applied on the DWT coefficients of HSI spectral bands. DWT is used to segment the HSIs into various sub-images, while TD is used to conserve the energy of the sub-images. Run Length Encoding (RLE) performs quantization of the component matrices and encoding of core tensors. The experiments are conducted with HSI compression based on DWT, TD with ALS method and HSI compression methods based on lossless JPEG (JPEG-LS), JPEG2000, Set Partitioning Embedded Block (SPECK), Object Based (OB)-SPEC and 3D-SPECK and the results of our work are found to be good in terms of Compression Ratio (CR) and Peak Signal-to-Noise Ratio (PSNR).

**Keywords:** ALS, CR, DWT, HSI, PSNR, RLE, TD.

Received June 17, 2013; accepted September 26, 2013; published online August 22, 2015

## 1. Introduction

Many military and civil applications involve the detection of an object or activity such as a military vehicle or vehicle tracks. Satellites must transmit a great amount of information to control on earth for its later processing. If the satellite carries out a preprocessing step in order to extract only the relevant information the communication process will be highly optimized.

Hyper Spectral Images (HSIs) are used in several applications such as soil analysis, forest monitoring, river flow analysis, environmental studies and other geographical analysis. HSI sensors are advanced digital color cameras with spectral resolution at a specific illumination wavelength. These sensors measure the radiation reflected by each pixel in a large no of visible or invisible frequency (or wavelength) bands. HSIs are considered as 3D data in compression methods known as third-order tensor, composing of two spatial dimensions and a spectral dimension. HSI applications are oriented toward classifying or grouping similar pixels, many instances of which are typical of each class of pixel since, interpretation of the scene is based on the clustering of the majority of pixels.

The compression of HSIs can be effected by detecting the spatial redundancies and spectral redundancies. The two main divisions of HSI compression methods are lossy compression and lossless compression. Lossless compression methods

are preferred in hyper spectral imaging because of the huge quantity of data and data loss must be negligible.

Many traditional compression algorithms for HSIs have only considered the spectral value in a feature space whose dimension were spectral bands. Basic compression methods for HSIs includes transform coding based algorithm, Vector Quantization (VQ) based algorithm, Differential Pulse Code Modulation (DPCM) algorithm and Adaptive DPCM (ADPCM). Some compression algorithms may increase the computational complexity and also lead to distortion. DPCM compression techniques involve expensive image decoder and multiple sampled signals rather than one.

The advantage of Discrete Wavelet Transform (DWT) is the temporal resolution in both frequency and time. The decomposition into sub-bands is highly flexible in terms of resolution scalability. Wavelets play a significant role in many image processing applications. Tucker Decomposition (TD) obtains a higher Compression Ratio (CR). This decomposition technique permits the allocation of any values for each dimension of the core tensor. TD is one of the most popular tensor decomposition methods for the compression of HSIs.

The proposed HSI compression algorithm is based on DWT and TD with Adaptive Least Squares (ALS) method. Applying 2DWT to each spectral band using biorthogonal wavelet will take care of the first stage compression by applying along the rows of the image

first and then the results are decomposed along the columns. TD is applied to the four wavelet sub-images to enhance the CR. The ALS method is used to compute the TD which is applied on the DWT coefficients of HSI spectral bands. Run Length Encoding (RLE) is used for the quantization of the component matrices and encoding of the elements of the core tensors.

The experiments were conducted for an HSI of the little Colorado River with the HSI compression based on DWT, TD with ALS method and existing HSI compression methods based on Lossless JPEG (JPEG-LS), JPEG2000, Set Partitioning Embedded Block (SPECK), Object Based (OB)-SPECK and 3D-SPECK and our work is found to be good in terms of CR and Peak Signal-to-Noise Ratio (PSNR).

The remaining part of the paper is organized as follows: Section 2 involves the works related to HSI compression techniques. Section 3 involves the generation of the three-dimensional HSI. Section 4 involves the detailed description of the DWT-TD (ALS)-RLE based HSI compression technique. Section 5 involves the performance analysis and comparison of the proposed HSI compression method and existing compression techniques based on JPEG-LS, JPEG2000, SPECK, OB-SPECK and 3D-SPECK. The paper is concluded in section 6.

## 2. Related Works

This section deals with the works related to recent HSI compression techniques. Hou *et al.* [13] proposed an HSI lossy-to-lossless compression using 3D Embedded ZeroBlock Coding (3D-EZBC) algorithm. This algorithm involves 3D transform based on spatial integer 2DWT and spectral integer 1D Karhunen-Loève Transform (1D-KLT). Context-based Adaptive Arithmetic Coding (AAC) and bit-plane zero-block coding are used for entropy coding. Lopez *et al.* [18] reviews the various reconfigurable hyper spectral imaging techniques in onboard systems. DWT is used to transform the HSI from the spatial domain to another domain and for both spatial and spectral decor relation. DWT-based compression techniques involve JPEG2000, Set Partitioning in Hierarchical Trees (SPIHT) and Embedded Zero-tree Wavelet (EZW). García-Vilchez *et al.* [9] the impact of lossy HSI compression is studied using supervised Support Vector Machine (SVM) classification and spectral unmixing. Here, DWT is used to decor relate the input HSI in the spatial domain.

Mažgut *et al.* [19] proposed a decomposition method of binary tensors. A Tucker model denoted as tensor-to-tensor projections are used for the decomposition of real tensors. The tucker model gives lesser reconstruction errors than the Parallel Factor analysis (PARAFAC) model. The tucker model is used as a link function and multi-linear predictor to correlate

the multi-linear predictions with the response variables. Shoham and Malah [21] used a Concatenative Text-To-Speech (CTTS) compressor for a larger acoustic database. This compressor employing 3D Shape-Adaptive Discrete Cosine Transform (3D-SADCT) can also be extended to hyper spectral imaging. Here, the coefficients of the 3D quantization matrix are coded using run-length encoding scheme.

Hendrix *et al.* [11] proposed an enclosing algorithm for abundance determination and end-member identification in HSIs. The noise in the HSI is minimized by a least squares method. Acevedo and Ruedin [2] proposed a lossless HSI compression technique employing dynamic Look-Up Tables (LUTs). A least squares estimator is used for the determination of scaling factor for the neighboring pixels in an HSI. In [1] a least-squares estimator was used to fasten the involved differential Huffman encoding.

The existing compression techniques employ encoding techniques like, JPEG-LS [25], Joint Photographic Experts Group (JPEG2000) [5], SPECK [22], 3D-SPECK [23], Lattice Vector Quantizer (LVQ)-SPECK [8], Discrete Wavelet Packet (DWP)-SPECK [8], Shape-Adaptive Reversible Integer Lapped Transform (SA-RLT) [16] and OB-SPECK [16]. Zhou *et al.* [27] designed uni-chip VLSI architecture for wireless image sensing. It involves Color Filter Array (CFA) preprocessing and JPEG-LS compression method. Song *et al.* [24] proposed a differential prediction and JPEG-LS based lossless HSI compression technique. Yin-Tsung *et al.* [26] proposed a lossless HSI compression method based on hardware/software code sign. The median predictor used in this model is defined in JPEG-LS format for intraband predication.

Lilian and Leila [17] review the data compression systems involved in satellite imagery. Lossless JPEG is basically a low complexity lossless compression for images. It consists of a modeling phase and an encoding phase. The encoding includes run length, differential coding, and Huffman code. Sriraam and Shyamsunder [23] proposed a 3D medical image compression involving multiple 3D wavelet coders. Four variants of daubechies and Cohen-Daubechies-Feauveau (CDF) wavelets are used in the first stage and encoders such as 3-D SPECK, 3-D SPIHT and 3-D BISK (binary set-partitioning using k-d trees) used in the second stage for the compression. Chang *et al.* [5] proposed a group and region based parallel HSI compression technique. This method employs a band clustering and signal subspace projection. A combination of Principal Component Analysis (PCA) and JPEG2000 are used to enhance the CR.

Wavelet coders such as SPECK and BISK are also used volumetric coding based EEG image compression [22]. They possess progressive resolution and quality during the compression process. Dutra *et al.* [8]

proposed a successive approximation wavelet coding for HSI compression. It involves two modules, first a LVQ codebook for processing of multiple samples and the next one is DWP-SPECK for DWP decomposition. DWP-SPECK involves 1D-DWT and simultaneous encoding of the huge number of spectral bands. Jiao *et al.* [16] proposed a lossless Region of Interest (ROI) coding for two-dimensional remote sensing images based on SA-RLT. This model can be a 3D model for HSIs by performing the following steps: Compute the SA-RLT in spatial domain, décor relate the spectral redundancy using integer DWT, and encode the transformed coefficients using 3D OB-SPECK or 3D OB-SPIHT. Rawat and Meher [20] introduced a hybrid image compression scheme (i.e., DCT and fractal image compression). The color image was compressed using DCT. Fractal image compression was employed for preventing the compression on the same blocks of the image.

### 3. Generation of 3D HSI

The source of an HSI is an imaging spectrometer which collects the images simultaneously in several spectral bands that can reach an approximately contiguous spectral sample. Higher amount of spectral bands increases the processing time and complexity. HSIs can be characterized as 3D data represented as:  $\underline{D}^{TMR^{S_1 \times S_2 \times S_3}}$ , where  $R^{S_1 \times S_2 \times S_3}$  is an  $S_1 \times S_2 \times S_3$  dimensional real vector space and  $S_1 \times S_2 \times S_3$  is the size of the HSI.

HSIs contain two types of simultaneous correlation namely, spectral correlation within the spectral bands and spatial correlation within the images. Generally, spectral correlation is higher than spatial correlation.

#### 3.1. 2DWT

DWT decomposes the signals into lower resolution with finer details. DWT consists of consecutive Low-Pass Filter (LPF) and High-Pass Filter (HPF). At each decomposition level, the HPF generates main information given as: Horizontal (H), Vertical (V) and Diagonal (D) information. The LPF affiliated with the scaling function generates the finer details represented as Approximate (A) information. 2DWT is applied to each band of HSIs. An image band comprises of  $S_1$  rows and  $S_2$  columns. On application of 2DWT four sub-band images namely  $A, H, V$  and  $D$ , each containing  $S_1/2$  rows and  $S_2/2$  columns are obtained. Images of sub-band  $A$  possess the highest energy among the coefficients of the remaining sub-band images, as shown in Figure 1.

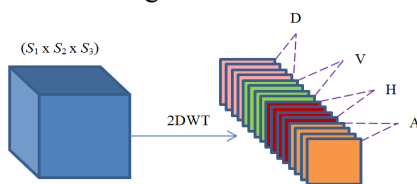


Figure 1. Decomposition of HSI.

The 2DWT of the function  $h(x, y)$  with size coordinates  $S_1$  and  $S_2$  is given in terms of coefficients as:

$$W_\varphi(s_1, s_2) = \frac{1}{\sqrt{S_1 S_2}} \sum_{y=0}^{S_2-1} \sum_{x=0}^{S_1-1} h(x, y) \varphi_{s_1, s_2}(x, y) \quad (1)$$

$$W_\psi^m(q, s_1, s_2) = \frac{1}{\sqrt{S_1 S_2}} \sum_{y=0}^{S_2-1} \sum_{x=0}^{S_1-1} h(x, y) \psi_{q, s_1, s_2}^m(x, y) \quad (2)$$

Here,  $m = \{H, V, D\}$ ,  $\varphi$  is the scaling function and  $\psi$  is the wavelet function. The coefficients  $W_\varphi(s_1, s_2)$  give an approximation of  $h(x, y)$ . The coefficients  $W_\psi(q, s_1, s_2)$  provide the H, V and D information. Conventionally,  $s_1 = s_2 = 2^q$  is selected so that  $q = 0, 1, \dots, Q-1$ . The functions  $\varphi_{s_1, s_2}(x, y)$  and  $\psi_{q, s_1, s_2}^m(x, y)$  are expressed in terms of wavelet filter coefficients  $c_\varphi$  and  $c_\psi$  respectively.

The wavelet filtering is performed by biorthogonal wavelet. The inverse 2DWT is calculated as:

$$h(x, y) = \frac{1}{\sqrt{S_1 S_2}} \sum_{s_2, s_1} W_\varphi(s_1, s_2) \varphi_{s_1, s_2}(x, y) + \frac{1}{\sqrt{S_1 S_2}} \sum_{m=\{H, V, D\}} \sum_{q=0}^{Q-1} W_\psi^m(s_1, s_2) \psi_{q, s_1, s_2}^m(x, y) \quad (3)$$

#### 3.2. Computation of TD

The third-order tensor  $\underline{A}^{TMR^{S_1 \times S_2 \times S_3}}$  is decomposed by TD into an unknown core tensor  $\underline{M}^{TMR^{Q_1 \times Q_2 \times Q_3}}$  multiplied by a set of component matrices  $A, B$  and  $C$ . The TD process is shown in Figure 2.

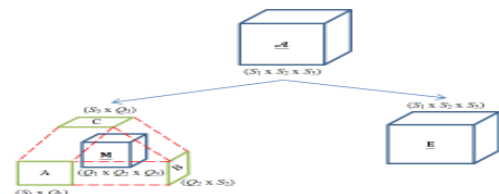


Figure 2. Third-order tensor decomposition by TD.

$$\underline{A} = \underline{M} \cdot A \cdot B \cdot C + \underline{E} = \hat{\underline{A}} + \underline{E} \quad (4)$$

Tensor  $\hat{\underline{A}}$  is an estimation of tensor  $\underline{A}$  and is dependent on the dimensions of the core tensor, i.e.,  $(Q_1, Q_2, Q_3)$ .  $\underline{E}$  gives the estimation error during the decomposition process.

ALS algorithm is used to compute the TDs and CANDECOMP (CANonical ECOMPosition)/PARAFAC (PARAFAC analysis) decompositions. This algorithm is adaptive in nature which in turn computes the TDs easily for dynamic tensors and suitable for higher order tensors.

The algorithm is provided for third order tensors and is stated in its general form as:

1. Given an order- $r$  tensor  $\hat{\underline{A}}$ , declare a set of projection matrices  $U^{(1)}, U^{(2)}, \dots, U^{(r)}$ .
2. Let  $ii = 1$ .

3. The equation for  $U^{(ii)}$  is solved keeping the other matrices constant.

The matricized form of  $A$  on mode  $i$  is represented as  $U^{(ii)}$ . It is equal to the product of two terms, where the first term is an  $n$ -ary Khatri-Rao product and the second term is a moore-penrose pseudo inverse. The aforementioned three steps are repeated for all  $ii$  from 1 to  $rr$  until convergence is attained.

While the above algorithm improves the convergence in all iterations, it is inefficient as it requires huge amount of required iterations for convergence.

The PARFAC components are generally estimated by the minimization of the quadratic cost function.

$$f(A, B, C) = \left\| \underline{M} - \sum_{r=1}^R a_r o b r c_r \right\|^2 \quad (5)$$

The minimization of Equation 5 involves two problems:

- The decomposition of core tensor  $M$  can be computed when Equation 5 becomes zero.
- The best rank  $R$  approximation to the core tensor  $\underline{M}$  can be calculated when the minimum of Equation 5 is distinct from zero.

Equation 5 is the generally minimized by the ALS algorithm in which the components are updated per mode. The components of the PARAFAC decomposition are  $2 \times 2 \times 2$  tensors. The tensors may be  $2 \times 2$  matrices or  $2 \times 3$  matrices, depending on the rank  $R$  of the tensor. The rank of the tensor is 1, 2 or 3. The component matrices are defined as:

$$A = (a_1, a_2, \dots, a_R) \quad (6)$$

$$B = (b_1, b_2, \dots, b_R) \quad (7)$$

$$C = (c_1, c_2, \dots, c_R) \quad (8)$$

With vectors  $a_i, b_i, c_i$  and  $i = 1, 2, \dots, R$  as columns. The quadratic cost function is rewritten as:

$$f(A, B, C) = \underline{M} - [A, B, C]^2 \quad (9)$$

ALS algorithm is used to solve Equation 9 as shown in the following steps:

- Initially, the ALS algorithm determines  $A$  under constant  $B$  and  $C$ .
- The component matrix  $B$  is updated under constant  $A$  and  $C$ .
- Once component matrix  $B$  is updated, component matrix  $C$  is updated under constant  $A$  and  $B$ .
- The updating process is repeated till a convergence criterion is satisfied.

### 4. Proposed Compression Method

TD decreases the spectral and spatial correlations simultaneously to enhance the  $CR$ . The flow of the proposed HSI compression based on DWT and TD

with ALS method is given in Figure 3.

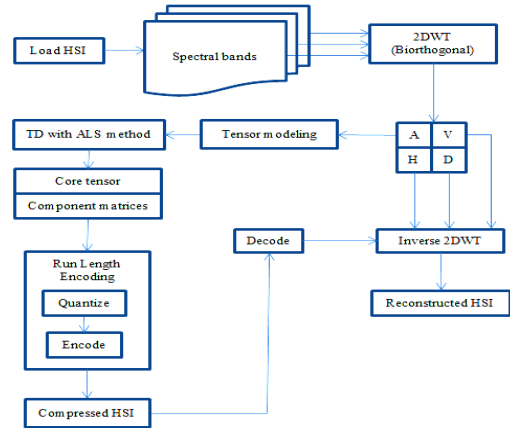


Figure 3. Working of proposed HSI compression based on DWT and TD with ALS method.

The HSI is simultaneously split into several spectral bands which are obtained from the imaging spectrometer. The HSI compression involves four stages. The first stage involves the application of biorthogonal wavelet based 2DWT to each band of HSIs to obtain four sub-band images ( $A, H, V, D$ ) for each spectral band. The tensor modeling process structures a tensor for each sub-band image ( $A, H, V, D$ ).

In the second stage, the four tensors are subjected to TD algorithm constructed upon the ALS method. The size of the core tensor is selected manually for each tensor. Tensor  $A$  contains the lowest frequency components with the majority of the wavelet coefficient energy. The values of ( $Q_{1A}, Q_{2A}, Q_{3A}$ ) are higher than those of other tensors. The values of ( $Q_{1D}, Q_{2D}, Q_{3D}$ ) are higher than the other remaining tensor values ( $Q_{1H}, Q_{2H}, Q_{3H}$ ) and ( $Q_{1V}, Q_{2V}, Q_{3V}$ ).

$CR$  is defined as the ratio of the number of bits in the original HSI to the number of transmitted bits. The number of transmitted bits is denoted as  $P$ .

$$CR = S_1 S_2 S_3 / P \quad (10)$$

$$P = \frac{S_1}{2} (Q_{1A} + Q_{1D} + Q_{1V} + Q_{1H}) + \frac{S_2}{2} (Q_{2A} + Q_{2D} + Q_{2V} + Q_{2H}) + S_3 (Q_{3A} + Q_{3D} + Q_{3V} + Q_{3H}) + Q_{1A} Q_{2A} Q_{3A} + Q_{1D} Q_{2D} Q_{3D} + Q_{1V} Q_{2V} Q_{3V} + Q_{1H} Q_{2H} Q_{3H} \quad (11)$$

The four core tensors for  $A, V, D, H$  and the component matrices for each core tensor are transmitted in the third stage. In the fourth stage, RLE performs quantization of the component matrices  $A, B, C$  and encoding of core tensors  $\underline{M}^{TMR} Q_1 \times Q_2 \times Q_3$ . The quantization process involves the compression of the data values in the component matrices to a single quantum value. The components in the frequency domain divide by a constant and then rounded to the nearest integer.

Each core tensor is scanned row-wise for determination of repetitive pixels and they are grouped. These groups contain the pixel value and the frequency of repetition. When a pixel value occurs only once it is not replaced with its frequency value as it would cause an overhead in compression. Consider the following

example in a core tensor:

Input Stream: 55 55 55 98 98 98 45 12 12 12 12

Encoded Stream: 355 498 45 412

The fifth stage involves the decoding of the transmitted compression data. The final sixth stage involves the inverse 2DWT for obtaining the reconstructed HSIs  $\hat{D}$ .

## 5. Performance Analysis

The experiments were conducted for an HSI of the little Colorado River with the proposed HSI compression method and existing HSI compression methods based on lossless JPEG [25], JPEG2000 [5], SPECK [22], 3D-SPECK [23] and OB-SPECK [16]. The performance of the compression techniques is analyzed and compared in terms of computational complexity, CR and PSNR.

### 5.1. Experimental Results

The HSI compression steps of the little Colorado River using the HSI compression method based on DWT-TD (ALS)-RLE is highlighted in Figure 4. The input HSI is loaded and is split into seven spectral bands. The DWT for band 7 of the input HSI with Level 1 decomposition is shown in Figure 5.

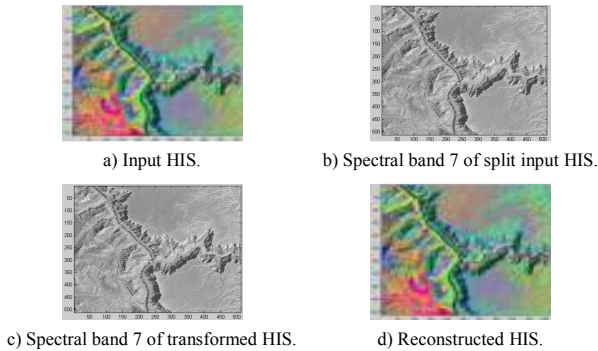


Figure 4. Compression steps for a HSI of little Colorado river.

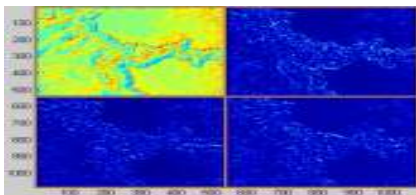


Figure 5. DWT for band 7 of HSI with level 1 decomposition.

### 5.2. Computational Complexity

The DWT of the proposed HSI compression technique involves biorthogonal wavelet and a unity decomposition level. This possesses a computational complexity of the order  $O(S_1S_2S_3)$ . The maximum computational complexity of TD is of the order  $O(Q_A S_A^3)$ , where  $S_A$  is the average number of pixels of the A tensor and  $Q_A$  is the average of the size dimensions of the A core tensor.

The total computational complexity of the (DWT-TD (ALS)-RLE) compressor is estimated as

$(O(Q_A S_A^3) + O(S_1 S_2 S_3))$ , whereas the computational complexity of HSI compression using DWT and TD alone resulted in a higher total computational complexity of  $(O(4Q_A S_A^3) + O(9S_1 S_2 S_3/7))$ , because it involves 4 core tensors and a (9/7) biorthogonal wavelet [15].

The computational complexities of existing HSI techniques like 3D-EZBC [13], Kronecker sensing [7], Iterative Spectral Mixture Analysis (ISMA) [14] and DWT-TD [15] are analyzed and compared in Table 1. 3D-EZBC and DWT-TD employed AVIRIS dataset images of low altitude and cuprite respectively [10]. Kronecker sensing used Smoothed Particle Hydrodynamics Code (SPHC) data cube [7]. ISMA method applied the splib06 dataset mentioned in [4]. It is observed that the DWT-TD (ALS)-RLE compression method performs satisfactorily in terms of computational complexity compared to the other existing methods.

Table 1. Performance analysis-computational complexity.

| Image/Data            | Method/Application | Computational Complexity            |
|-----------------------|--------------------|-------------------------------------|
| Low Altitude          | 3D-EZBC            | $O(S_1^2) + O(2(S-2)) + O(S-2)$     |
| Cuprite               | DWT-TD             | $O(4Q_A S_A^3) + O(9S_1 S_2 S_3/7)$ |
| SPHC data cube        | Kronecker sensing  | $O(S_1 \log S_1)$                   |
| splib06               | ISMA               | $O((S_1 S_2 S_3)^3)$                |
| Little Colorado River | Our work-Avg.      | $O(Q_A S_A^3) + O(S_1 S_2 S_3)$     |

### 5.3. Compression Ratio

The CR of the existing JPEG-LS compression [25] and the DWT-TD ALS-RLE compression is analyzed and compared for four HSI datasets in Figure 6. CR for HSI-1 in our work is significantly higher than that of JPEG-LS compression. Then, CR decreases gradually in our work compared to JPEG-LS compression, for datasets HSI-2, HSI-3 and HSI-4. It is observed that on an average basis CR for the DWT-TD ALS-RLE compression is slightly higher than that of JPEG-LS compression. The small rise in CR for the proposed compression over JPEG-LS compression is because they are only lossless compression techniques concentrating mainly on conservation of the huge data.

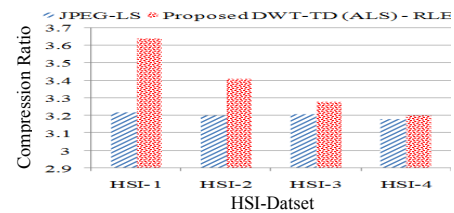


Figure 6. CRs of JPEG-LS compression and DWT-TD ALS-RLE compression.

CR obtained by other researchers using techniques like wireless image sensors [27], differential prediction [24] and lossless interceding [5] are analyzed and compared with DWT-TD (ALS)-RLE compression in Table 2. These methods employed compression methods like least squares, JPEG-LS and JPEG2000. They employed test images like Airplane [3], polar iris images [12], etc., the test image files were also, taken in BIL (Band Interleaved by Line) format and BSQ (band Sequential) format. The comparative analysis

showed that the CR of DWT-TD (ALS)-RLE compression is better compared to other techniques.

Table 2. Performance analysis-CR.

| Image/Data            | Method/Application               | Main Focus        | CR   |
|-----------------------|----------------------------------|-------------------|------|
| Airplane              | Wireless Image Sensor            | JPEG-LS           | 2.99 |
| Avg. -BIL, BSQ        | Differential Prediction-Spatial  | JPEG-LS           | 2.51 |
| Avg. -BIL, BSQ        | Differential Prediction-Spectral | JPEG-LS           | 2.66 |
| CASIA V1              | Polar Iris                       | JPEG2000          | 2.42 |
| Party Scene           | Lossless Intra Coding            | JPEG-LS           | 1.79 |
| Little Colorado River | Our Work-Avg.                    | DWT-TD (ALS)- RLE | 3.38 |

### 5.4. PSNR

PSNR (dB) is the ratio of the maximum possible power of input HSI to the power of error introduced by the compression. The quality of the reconstructed HSI is higher when the PSNR is higher. The quality metric analysis for the DWT-TD ALS-RLE compression in terms of PSNR for the seven bands of input HSI is given in Figure 7. It is observed that the PSNR value varies between 31.1dB and 32.1dB. The maximum PSNR value is obtained in the band 6 of the input HSI and minimum PSNR value is obtained in the band 2 of the input HSI.

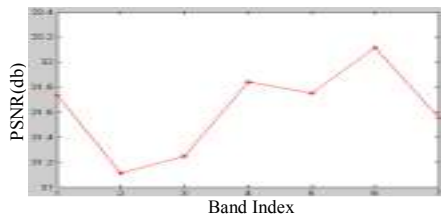


Figure 7. Quality metric analysis for the DWT-TD ALS-RLE in terms of PSNR.

The PSNR values of the existing 3D-SPECK compression [23] and DWT-TD ALS-RLE compression is analyzed and compared for five HSI datasets in Figure 8. PSNR for HSI-1 in the case of proposed compression is significantly higher than that of 3D-SPECK compression. Then, CR increases gradually in the case of the 3D-SPECK compared to DWT-TD ALS-RLE compression, for datasets HSI-2, HSI-3, HSI-4 and HSI-5. It is observed that on an average basis PSNR for the DWT-TD ALS-RLE compression is higher than that of JPEG-LS compression by approximately 5.96dB.

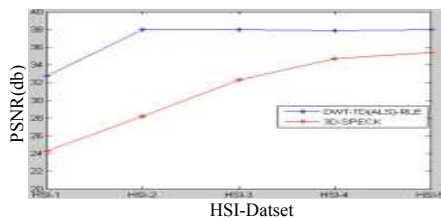


Figure 8. PSNR values for DWT-TD ALS-RLE compression and 3D-SPECK compression.

PSNR obtained by other researchers using techniques like volumetric coding [22], JPEG2000-ROI [16] and OB-SPECK [16] are analyzed and compared with DWT-TD ALS-RLE compression in

Table 3. These methods employed compression methods like JPEG2000 [16], SPECK [24], SA-RLT [16] and SA-DWT [16]. They employed test images like motor movement imagery and Shelter Island-BG (Background) and ROI. The comparative analysis showed that the PSNR of DWT-TD ALS-RLE compression is better compared to other techniques.

Table 3. Compression of PSNR.

| Method/Application | Main Focus        | Image/Data                     | PSNR (dB) |
|--------------------|-------------------|--------------------------------|-----------|
| Volumetric Coding  | SPECK             | Motor movement- Avg. step size | 34.26     |
| JPEG2000- ROI      | JPEG2000          | Shelter Island- ROI            | 32.49     |
| OB-SPECK           | SA-DWT            | Shelter Island- BG             | 27.12     |
| OB-SPECK           | SA-RLT            | Shelter Island- ROI            | 34.39     |
| OB-SPECK           | SA-RLT            | Shelter Island- BG             | 27.72     |
| Our Work-Avg.      | DWT-TD (ALS)- RLE | Little Colorado River          | 36.67     |

### 6. Conclusions

The proposed HSI compression based on DWT, TD with ALS method reduces the size of the 3D tensors calculated from the four wavelet sub-images of the spectral bands of HSIs. The experiments were conducted for an HSI of the little Colorado River with the HSI compression based on DWT, TD with ALS method and existing HSI compression methods based on JPEG-LS, JPEG2000, SPECK, OB-SPECK and 3D-SPECK and our work was found to be good in terms of CR and PSNR value. The future work involves the development of RLE and simplification of the tensor calculations to decrease the memory consumption, computational load and processing time for the HSI compression.

### References

- [1] Abrardo A., Barni M., Magli E., and Nencini F., "Error-Resilient and Low-Complexity Onboard Lossless Compression of Hyperspectral Images by Means of Distributed Source Coding," *IEEE Transactions on Geoscience and Remote Sensing*, vol. 48, no. 4, pp. 1892-1904, 2010.
- [2] Acevedo D. and Ruedin A., "Lossless Compression of Hyperspectral Images: Look-Up Tables with Varying Degrees of Confidence," *in Proceedings of IEEE International Conference on Acoustics Speech and Signal Processing*, Dallas, pp. 1314-1317, 2010.
- [3] Anonymous, The USC-SIPI Image Database-Volume 3: Miscellaneous., available at: <http://sipi.usc.edu/database/database.php?volume=misc>, last visited 2013.
- [4] Anonymous2008, USGS Digital Spectral Library 06., available at: <http://speclab.cr.usgs.gov/spectral.lib06/ds231/>, last visited 2013.
- [5] Cai Q., Song L., Li Guichun., and Ling N., "Lossy and Lossless Intra Coding Performance Evaluation: HEVC, H.264/AVC, JPEG 2000 and JPEG LS," *in Proceedings of Signal and Information Processing Association Annual*

- Summit and Conference*, Hollywood, pp. 1-9, 2012.
- [6] Chang L., Chang y., Tang Z., and Huang B., "Group and Region based Parallel Compression Method using Signal Subspace Projection and Band Clustering for Hyperspectral Imagery," *IEEE Journal of Selected Topics in Applied Earth Observations and Remote Sensing*, vol. 4, no. 3, pp. 565-578, 2012.
- [7] Duarte M. and Baraniuk R., "Kronecker Compressive Sensing," *IEEE Transactions on Image Processing*, vol. 21, no. 2, pp. 494-504, 2012.
- [8] Dutra A., Pearlman W., and Silva E., "Successive Approximation Wavelet Coding of AVIRIS Hyperspectral Images," *IEEE Journal of Selected Topics in Signal Processing*, vol. 5, no. 3, pp. 370-385, 2011.
- [9] García-Vílchez F., Muñoz-Marí J., Zortea M., Blanes I., González-Ruiz V., Camps-Valls G., Plaza A., and Serra-Sagristà J., "On the Impact of Lossy Compression on Hyperspectral Image Classification and Unmixing," *Geoscience and Remote Sensing Letters*, vol. 8, no. 2, pp. 253-257, 2011.
- [10] Gowey K. and S Al., "AVIRIS Data-Ordering Free AVIRIS Standard Data Products," available at: [http://aviris.jpl.nasa.gov/data/free\\_data.html](http://aviris.jpl.nasa.gov/data/free_data.html), last visited 2013.
- [11] Hendrix E., García I., Plaza J., Martin G., and Plaza A., "A New Minimum-Volume Enclosing Algorithm for Endmember Identification and Abundance Estimation in Hyperspectral Data," *IEEE Transactions on Geoscience and Remote Sensing*, vol. 50, no. 7, pp. 2744-2757, 2012.
- [12] Horvath K., Stögner H., Uhl A., and Weinhandel G., "Lossless Compression of Polar Iris Image Data," in *Proceedings of the 5<sup>th</sup> Iberian Conference*, Spain, pp. 329-337, 2011.
- [13] Hou Y. and Li Y., "Hyperspectral Image Lossy-to-Lossless Compression using 3D SPEZBC Algorithm Based on KLT and Wavelet Transform," in *Proceedings of the 2<sup>nd</sup> Sino-foreign-interchange Workshop*, China, pp. 713-721, 2012.
- [14] Iordache M., Bioucas-Dias J., and Plaza A., "Sparse Unmixing of Hyperspectral Data," *IEEE Transactions on Geoscience and Remote Sensing*, vol. 49, no. 6, pp. 2014-2039, 2011.
- [15] Karami A., Yazdi M., and Mercier G., "Compression of Hyperspectral Images using Discrete Wavelet Transform and Tucker Decomposition," *IEEE Journal of Selected Topics in Applied Earth Observations and Remote Sensing*, vol. 5, no. 2, pp. 444-450, 2012.
- [16] Jiao L., Wang L., Wu J., Bai J., Wang S., and Hou B., "Shape-Adaptive Reversible Integer Lapped Transform for Lossy-to-Lossless ROI Coding of Remote Sensing Two-Dimensional Images," *IEEE Geoscience and Remote Sensing Letters*, vol. 8, no. 2, pp. 326-330, 2011.
- [17] Lilian N. and Leila F., "Performance evaluation of Data Compression Systems Applied to Satellite Imagery," *Journal of Electrical and Computer Engineering*, vol. 2012, no. 18, pp. 1-15, 2012.
- [18] Lopez S., Vadimirova T., Gonzalez C., Resano J., Mozos D., and Plaza A., "The Promise of Reconfigurable Computing for Hyperspectral Imaging Onboard Systems: A Review and Trends," *Proceedings of the IEEE*, vol. 101, no. 3, pp. 698-722, 2013.
- [19] Mazgut J., Tino P., Boden M., and Yan H., "Dimensionality Reduction and Topographic Mapping of Binary Tensors," *Pattern Analysis and Applications*, vol. 17, no. 3, pp. 1-19, 2013.
- [20] Rawat M. and Sukadev S., "A Hybrid Image Compression Scheme using DCT and Fractal Image Compression," *the International Arab Journal of Information Technology*, vol. 10, no. 6, pp. 553-562, 2013.
- [21] Shoham T., Malah D., and Shechtman S., "Quality Preserving Compression of a Concatenative Text-To-Speech Acoustic Database," *IEEE Transactions on Audio, Speech, and Language Processing*, vol. 20, no. 3, pp. 1056-1068, 2012.
- [22] Srinivasan K., Dauwels J., and Reddy M., "Multichannel EEG Compression: Wavelet-Based Image and Volumetric Coding Approach," *IEEE Journal of Biomedical and Health Informatics*, vol. 17, no. 1, pp. 113-120, 2013.
- [23] Sriraam N. and Shyamsunder R., "3-D Medical Image Compression using 3-D Wavelet Coders," *Digital Signal Processing*, vol. 21, no. 1, pp. 100-109, 2011.
- [24] Song H., Song Z., Deng G., Ma Y., Ma P., "Differential Prediction-Based Lossless Compression with Very Low-Complexity for Hyperspectral Data," in *Proceedings of the 13<sup>th</sup> International Conference on Communication Technology*, Jinan, pp. 323-327, 2011.
- [25] Wahl S., Haitham A., Tantawy H., Wang Z., Werner P., and Simon S., "Exploitation of Context Classification for Parallel Pixel Coding in JPEG-LS," in *Proceedings of the 18<sup>th</sup> International Conference on Image Processing*, Brussels, pp. 2001-2004, 2011.
- [26] Yin-Tsung Y., Cheng-Chen H., and Ruei-Ting L., "Lossless Hyperspectral Image Compression System-based on HW/SW Codesign," *Embedded Systems Letters*, vol. 3, no. 1, pp. 20-23, 2011.
- [27] Zhou R., Liu L., Yin S., Luo A., Chen X., and Wei S., "A VLSI Design of Sensor Node for Wireless Image Sensor Network," in *Proceedings*

of *IEEE International Symposium on Circuits and Systems*, Paris, pp. 149-152, 2010.



**Kala Rajan** is Associate Professor in Sri Subramanya College of engineering and technology, Palani, Tamilnadu, India. She holds M.E degree in Applied Electronics in Anna University, Trichy and she is a fellow membership of MISTE. She has also, completed her master degree in business administration in the year 2002. She has more than 11 years of experience including extensive project management experience in planning and leading a range of Electronic projects during these years, she shouldered a number of teachings, and societal based assignments. She also leads and teaches modules at both BE and ME levels in electronics and communication



**Vasuki Murugesan** completed her PhD degree in Color Image Processing from Anna University, Chennai. Presently, she is working as Professor and Head in Electronics and Communication Engineering Department at Velammal College of Engineering and Technology, Madurai, Tamilnadu, India. She has 26 years of teaching experience. Her research interests are in computer vision, wavelet based image analysis, bio medical image processing and pattern recognition schemes. She has published 30 papers in International Journals and presented 200 papers in International and National conferences. She is a Life Member of Indian Society of Technical Education (ISTE) and Fellow member of Institution of Electronics and Telecommunication Engineers (IETE) and Member in IEEE.